ANGULAR RECONSTITUTION: A POSTERIORI ASSIGNMENT OF PROJECTION DIRECTIONS FOR 3D RECONSTRUCTION

Marin VAN HEEL

Fritz Haber Institute of the Max Planck Society, Faradayweg 4–6, D-1000 Berlin Dahlem, Germany

In computerized tomography as well as in most problems of three-dimensional reconstruction from projections, one knows from the experimental set-up the angular relationships between the projections from which the reconstruction is to be calculated. A serious difficulty is encountered when the angles are not known. In this paper, a method of "angular reconstitution" is described, which allows the a posteriori determination of the relative angular orientations of the projections and thus enables the three-dimensional reconstruction of the object to be calculated. For asymmetric objects, a minimum of three projections is required, which should not be related by a tilt around a single rotation axis. The method can be applied to determine the three-dimensional structure of biological macromolecules based on electron micrographs of randomly oriented individual molecules. Angular reconstitution, in combination with multivariate statistical techniques to classify and average the characteristic views of a molecule forms a complete, self-contained methodology for molecular structure analysis by electron microscopy.

1. Introduction

Three-dimensional (3D) reconstruction of an object from its two-dimensional (2D) projections is a well established technique used routinely in various fields including medicine, astronomy and electron microscopy (for reviews see references [1–5]). A prerequisite for virtually all published 3D reconstruction techniques is knowledge of the relative angular orientations of the projections in terms of the three Eulerian angles α, β and γ (defined in appendix). When the projections are related to each other by a rotation around a common tilt axis ("tomography" as opposed to "direct 3D"), knowledge of only one tilt angle is required. In medical computerized X-ray tomography, for example, a projection source is rotated around the patient using typically one-degree intervals between successive projections (c.f. ref. [1]). In electron microscopy, the specimen can be tilted over known though restricted angles relative to the electron beam to generate the different projections [2–9]. In both situations, the orientational information is clearly available.

In typical electron microscopical preparations of single biological macromolecules, the macromolecules can assume various stable positions on the support film depending on their shape and adsorption properties. Multivariate statistical data compression [10,11] and classification techniques [12] can be used to sort and partition a large set of noisy macromolecular images, giving averages of the different characteristic views [13] with an enhanced signal-to-noise ratio (SNR). These characteristic views represent projections of the object in different directions. The absence of orientational information prevents the immediate application of reconstruction algorithms to obtain the 3D structure. This problem motivated the current study, which was first presented at the 1986 EMSA annual meeting in Albuquerque.

2. Reconstitution of projection directions

2.1. Angular reconstitution concepts

Almost all algorithms for 3D reconstruction from projections are based in one way or another on the well known central section or projection theorem [14–16]. It states that the Fourier transform of any 2D projection of a 3D density distribution is a 2D section through the center of the 3D Fourier transform of the 3D density distribution. The 2D central section is perpendicular to the projection direction in real space; the projection direction thus coincides with the normal of the central section plane. If we have two different projections of the same structure, we have two corresponding central sections which will necessarily have one central line in common [17,18] (fig. 1). When all projections to be considered stem from a single tilt axis experiment, they all share the same central line, which is equivalent to the tilt axis of the experiment. The 3D reconstruction problem can then be solved in all 2D slices perpendicular to the tilt axis independently ("tomography"). Here, however, the interest lies in "direct 3D" reconstructions for which there will be no common axis.

The central section theorem can also be formulated – a dimension lower – as a "central line theorem" for two-dimensional density distribution: a 1D projection (line projection) of a 2D density is equivalent to a 1D central line through the 2D Fourier transform of the 2D density distribution, and vice versa. The fact that two central sections have one central line in common, in conjunction with the central line theorem, can be formulated equivalently in real space: two 2D projections of the same 3D object will always have one 1D or line projections in common. The term "common tilt axis" is appropriate for this common line projection. The common tilt axis between the two projections is perpendicular to the projection directions of both projections. The existence of the common tilt axis can be proved directly without a detour through Fourier space. The formal equivalence of different concepts in real space and in Fourier space is shown in the diagram of fig. 2.
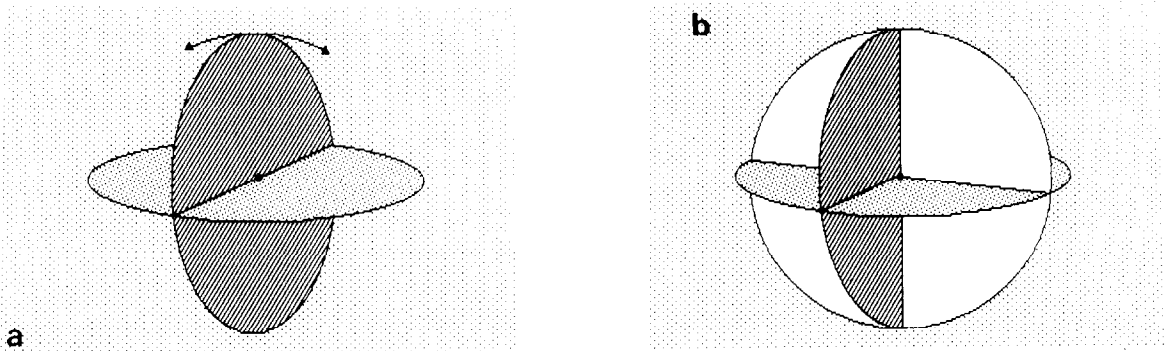

Fig. 1a. Two projections of a 3D object correspond to two central (through the origin) sections in 3D Fourier space which share one common central line. The projection directions are parallel to the normals of the central section planes. The common central line is equivalent to the real-space common tilt axis of the two projections. This common tilt axis does not fully fix the spatial orientation of the two projections, since a relative rotation of the central sections around the common tilt axis remains possible. The common tilt axis can be determined as described in the text.

Fig. 1b. Introducing a third central section in the system depicted in fig. 1a, gives two more common lines and fixes the relative spatial orientation of all three central sections, and therewith of the three projection directions which are perpendicular to the central section planes. The only ambiguity that remains is that of the handedness of the object: a right- and a left-handed combination of the central sections are both correct solutions to the angular reconstitution problem.
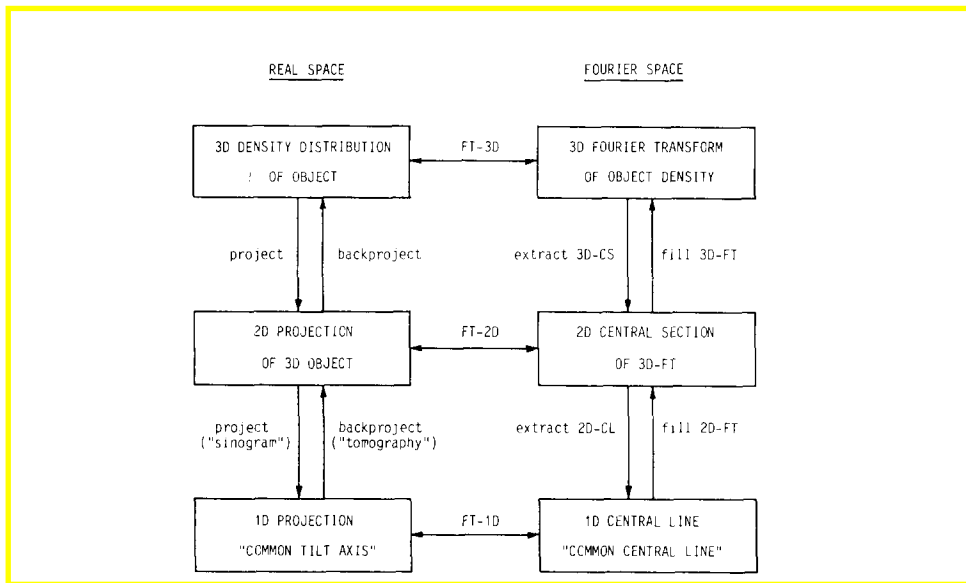
REAL SPACE - FOURIER SPACE EQUIVALENCE

REAL SPACE   FOURIER SPACE

| 3D DENSITY DISTRIBUTION OF OBJECT | FT-3D | 3D FOURIER TRANSFORM OF OBJECT DENSITY |

project   backproject   extract 3D-CS   fill 3D-FT

| 2D PROJECTION OF 3D OBJECT | FT-2D | 2D CENTRAL SECTION OF 3D-FT |

project   backproject   extract 2D-CL   fill 2D-FT
("sinogram")   ("tomography")

| 1D PROJECTION "COMMON TILT AXIS" | FT-1D | 1D CENTRAL LINE "COMMON CENTRAL LINE" |

Fig. 2. The formal equivalence between various real space and Fourier space operations is shown schematically in this diagram. Abbreviations used: CL = central line, CS = central section, FT = Fourier transform.

Although the common tilt axis of the two projections is fixed, a rotation of the two projections, relative to each other, around that axis remains possible. This last degree of freedom disappears when a third projection is introduced into the system (fig. 1b). The third projection will have a common tilt axis with the first projection and a different common tilt axis with the second projection. The total of three different common tilt axes will fix the spatial orientation of the system, provided that the three tilt axes are indeed different, that is, the three projections may not be related by one single common tilt axis.

2.2. A simple example

The method may be demonstrated using a simple model consisting of 12 balls in D6 symmetry [19] (fig. 3a), although the symmetry property is not exploited here. From the 3D model, three different 2D projections (labelled 1, 2 and 3) are calculated (fig. 3). In this simple example, the common lines can immediately be identified. In figs. 3b–3d, the projections are mounted such that common line projections (drawn schematically in the images) of pairs of (projection) images are parallel to each other. For complex objects, we find the common tilt axis between each pair of projections by the technique discussed below.

The basic idea then is that from each of these 2D projections, we can determine the two common tilt axes relative to the two other 2D projection images, and that we thus can determine the angle between these common tilt axes. For example, if we call the common tilt axis between projection 1 and projection 2 "$\hat{C}_{12}$" and between projections 1 and 3 "$\hat{C}_{31}$"; we can determine the angle A: $\angle A = \angle (\hat{C}_{31}, \hat{C}_{12})$, as well as $\angle B = \angle (\hat{C}_{12}, \hat{C}_{23})$ and $\angle C = \angle (\hat{C}_{23}, \hat{C}_{31})$ (see figs. 3b–3d). This total of three angles fixes the relative spatial orientation of the system as indicated in fig. 1b. The way in which these three directions are fixed in space is described by the already ancient science of spherical trigonometry (cf. ref. [20]). Here, however, we will use a vector and matrix approach to derive the necessary formulas.
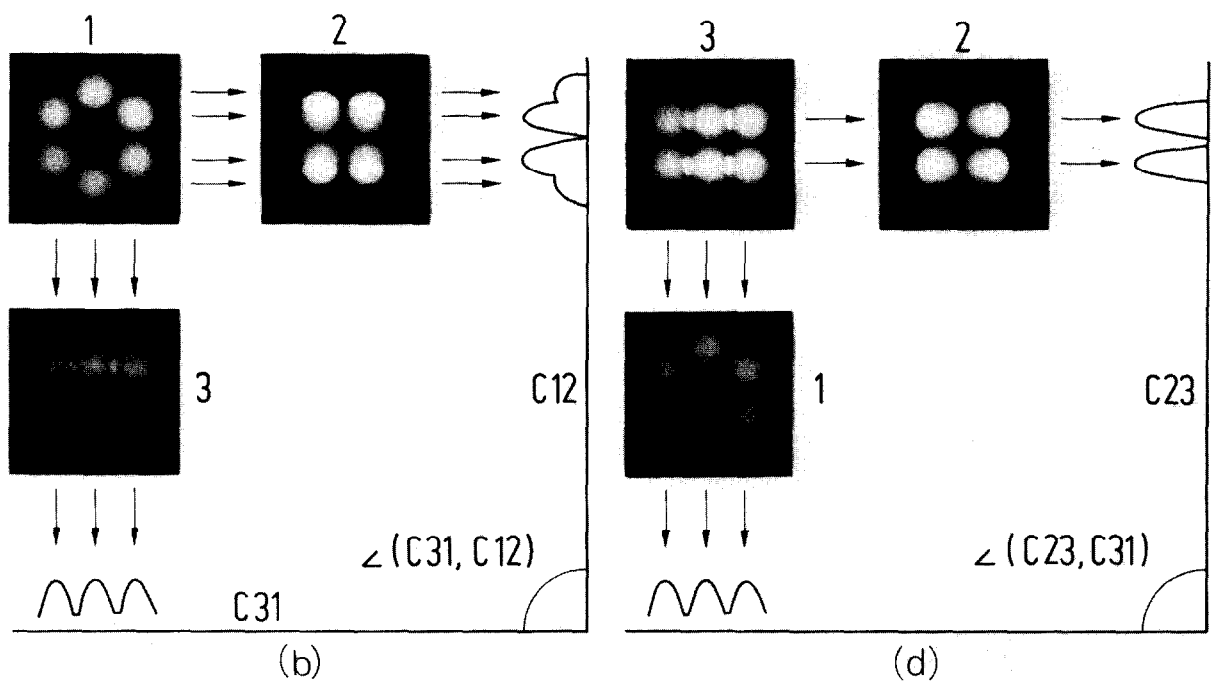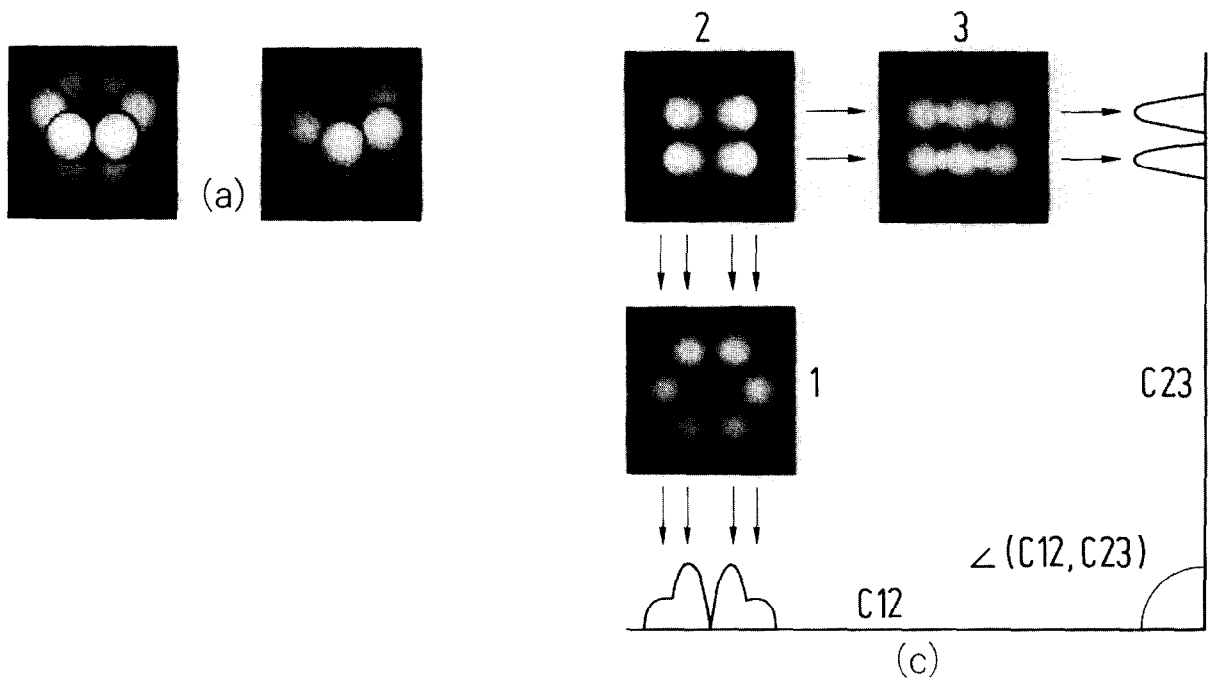
(a)

(b)

(c)

(d)

Fig. 3a. A 3D model density was generated consisting of 12 balls in a D6 pointgroup arrangement. The model was projected into three different projection directions giving three different 2D projections of the model. The projection directions were chosen to lie along the main symmetry axes for didactical reasons. The shaded surface of the model is shown here twice, as seen from directions that are 30° away from the two different two-fold axes and 60° away from the six-fold axis of the D6 structure.

Fig. 3b–3d. Three different projection directions are labeled 1, 2, and 3. It is clear that certain line (1D) projections of each of the 2D projections are identical. These line projections are shown schematically. The arrangement in figs. 3b–3d is such that the common line projections (common tilt axes) of the different 2D projections (called C_{12} and C_{31}) are parallel to each other. From this combination of three projection we can extract the angle A between C_{12} and C_{31} ($\angle A = \angle(C_{31}, C_{12})$). The remaining angles $B(\angle B = \angle(C_{12}, C_{23}))$ (fig. 3c) and C ($\angle C = \angle(C_{23}, C_{31})$) (fig. 3d) can be determined equivalently from the other possible combinations of projections.
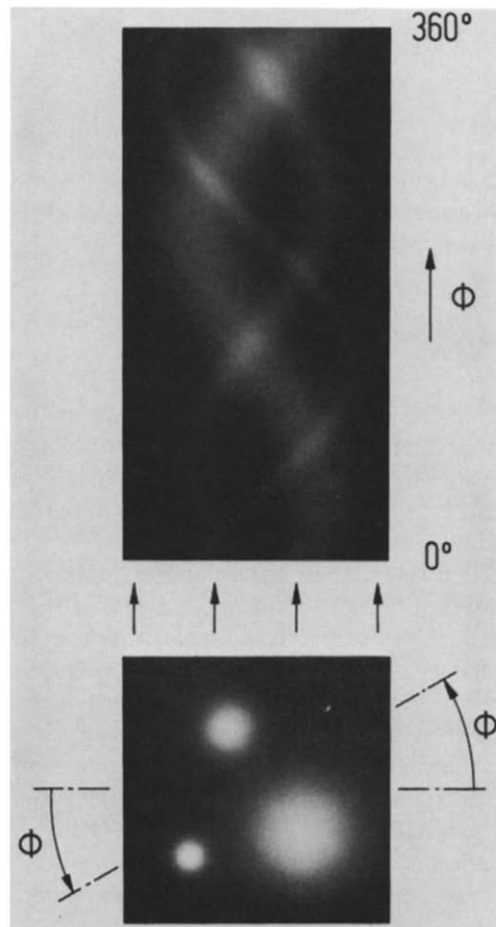

Fig. 4. Illustration of a sinogram calculation. Line projections are calculated for incrementing angular directions. These line projections are then mounted one after the other as the rows of a 2D image. The name sinogram comes from the sine waves that appear in the sinogram when characteristic spots of the original image are projected in all directions. The 2D image used here consists of three simple blobs of different size. Each line in the sinogram image in the illustration is the line projection of the blobs image in the upward direction, after rotation of the image over an angle ϕ. The lower half of the sinogram is identical to the mirrored top half, since this sinogram was calculated over the full 0–360° range.
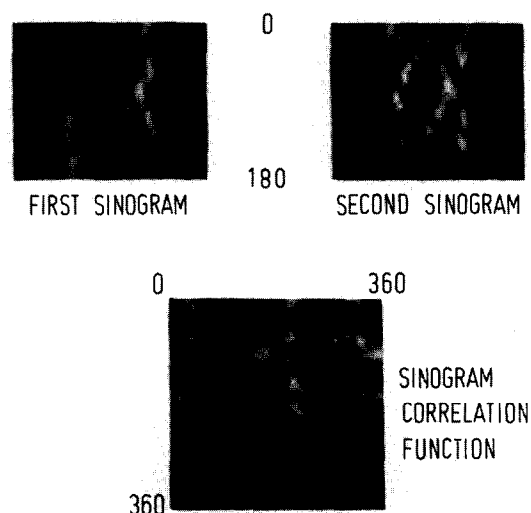
Fig. 5. From two sinograms, taken from a practical application (work in preparation), a sinogram-correlation function (SCF) is generated by correlating two sinogram lines at a time; from each such comparison, one SCF value is obtained. Each sinogram is normally calculated over a 0–180° range; the SCF is calculated over the full 0–360° range such that the SCF becomes cyclical in both directions. This, in turn, facilitates the peak searching using a least-squares paraboloid shape fitting procedure.

2.3. Finding the common tilt axes: computational procedure

Starting with a set of three projection images, the first step in the angular reconstitution procedure is to search for the common tilt axis or common line projection between each given pair of projections. For this purpose we first calculate all possible line (1D) projections of each 2D projection of the object. The line projections are normally calculated over a 180° range at typically 1° to 3° intervals; these projection lines can be displayed as a 2D image known as a "sinogram" (fig. 4).

All sinograms are then compared pairwise in the following manner. The crosscorrelation coefficient between each line of the first and each line of the second sinogram are computed, after normalization of the sinogram lines to a standard variance value. This normalization is performed so that the correlation coefficient becomes a more reliable measure of similarity between line projections. All correlation coefficients between the first line of the first sinogram and all lines of the second sinogram are then used to fill the first line of a sinogram correlation function (SCF); the second line of this two-dimensional function (or image) is filled with the correlation coefficient values of the second line of the first sinogram with respect to all lines of the second sinogram, etc. An example of an SCF is shown in fig. 5. We apply to this image a least-squares fitting procedure with a paraboloid function over an environment of the largest peak(s) so as to obtain the orientation of the common tilt axis between the two projections more precisely.

The search for the common line(s) can equally well be performed in Fourier space [17,18]. The only disadvantage is that the Fourier space equivalent of the sinogram, a sequence of central lines through a 2D Fourier transform, is a complex function and is therefore not as easy to visualize. At the level of the final SCF, however, the differences between real and Fourier space analyses disappear altogether since identical functions are obtained. Independent of whether the search is performed in Fourier space or in real space, the result of the search, for a three-projection system, is a set of three angles between the three common lines of the system.

2.4. Calculation of Euler angles α and β

The relative orientations of the three projections are fixed. Yet, the absolute orientation of the object relative to the $X-Y-Z$ coordinate system is arbitrary and may thus be chosen freely. For simplicity, we choose the common tilt axis (or common line) $\hat{C}_{12}$ between projections 1 and 2 to coincide with the Z-axis. The general expression for a common tilt axis $\hat{C}_{ij}$ between projection "i" and projection "j" is (appendix):

$$\hat{C}_{ij} = \begin{pmatrix} \sin \beta_{ij} \cos \alpha_{ij} \\ \sin \beta_{ij} \sin \alpha_{ij} \\ \cos \beta_{ij} \end{pmatrix}. \tag{1}$$

For the Z-axis we have $\alpha_{12} = 0°$ and $\beta_{12} = 0°$, such that the $\hat{C}_{12}$ direction vector becomes:

$$\hat{C}_{12} = \begin{pmatrix} 0 \\ 0 \\ 1 \end{pmatrix}. \tag{2}$$

Next, we choose the common line between projection 3 and 1 ($\hat{C}_{31}$) to lie in the $Y-Z$ plane (i.e. $\alpha_{31} = 90°$); this implies that we choose the first projection direction to be the direction of the X-axis (the projection $\hat{D}_1$ is given by the outer product of $\hat{C}_{12}$ and $\hat{C}_{31}$). We thus have for $\hat{C}_{31}$:

$$C_{31} = \begin{pmatrix} 0 \\ \sin \beta_{31} \\ \cos \beta_{31} \end{pmatrix}. \tag{3}$$

For the third common tilt axis, $\hat{C}_{23}$, we still have:

$$\hat{C}_{23} = \begin{pmatrix} \sin \beta_{23} \cos \alpha_{23} \\ \sin \beta_{23} \sin \alpha_{23} \\ \cos \beta_{23} \end{pmatrix}. \tag{4}$$

The primary measurable quantities are the angles between the common tilt axes; with $\hat{C}_{12}$ being identical to the Z-axis, we have two very simple inner product relations:

$$\cos A = \hat{C}_{31} \cdot \hat{C}_{12} = \cos \beta_{31}, \quad \cos B = \hat{C}_{12} \cdot \hat{C}_{23} = \cos \beta_{23}. \tag{5}$$

And, equivalently:

$$\cos C = \hat{C}_{23} \cdot \hat{C}_{31} = \sin \beta_{23} \sin \alpha_{23} \sin \beta_{31} + \cos \beta_{23} \cos \beta_{31}. \tag{6}$$

It is not surprising that this last formula has a more than superficial similarity to the "cosine rule" of spherical trigonometry [20]. Since in this relation everything except $\sin \alpha_{23}$ is known, we can solve for $\sin \alpha_{23}$ and therewith the spatial orientations of $\hat{C}_{12}$, $\hat{C}_{23}$ and $\hat{C}_{31}$ are known. However, from these equations two correct but essentially different solutions for the common lines can be obtained: a left- and a right-handed combination. The handedness of a combination of three (unit) vectors (a "tripod") can be determined from the determinant of the matrix consisting of the three vectors; for our combination of $\hat{C}_{12}$, $\hat{C}_{23}$ and $\hat{C}_{31}$, we have:

$$D = \begin{vmatrix} 0 & \sin \beta_{23} \cos \alpha_{23} & 0 \\ 0 & \sin \beta_{23} \sin \alpha_{23} & \sin \beta_{31} \\ 1 & \cos \beta_{23} & \cos \beta_{31} \end{vmatrix} = \sin \beta_{23} \cos \alpha_{23} \sin \beta_{31}. \tag{7}$$

With the angular reconstitution method it is thus not possible to directly determine the absolute handedness of the reconstructed object [21]. Having determined the common lines between the projections, the projection directions $\hat{D}_1$, $\hat{D}_2$ and $\hat{D}_3$ are obtained from the outer product relations:

$$\hat{D}_1 \sim \hat{C}_{31} \times \hat{C}_{12}, \quad \hat{D}_2 \sim \hat{C}_{12} \times \hat{C}_{23}, \quad \hat{D}_3 \sim \hat{C}_{23} \times \hat{C}_{31}. \tag{8}$$

These direction vectors uniquely determine the desired Euler angles α and β (through eq. (A.7)).

2.5. Calculation of the Euler angle γ

The angles of the various projections determine how these projections have to be rotated in the plane before they enter the 3D reconstruction. Since we have chosen the $\hat{C}_{12}$ common line to be in the same direction as the Z-axis, the angles of the first and the second projection directions, γ_1 and γ_2, are fixed by that choice. The angle γ_3, however, still has to be determined. For this purpose, we calculate where in the local coordinate system of projection 3 the common line $\hat{C}_{31}$ lies, which in the normal coordinate system ($\alpha_{31} = 90°$) is:

$$\hat{C}_{31} = \begin{pmatrix} 0 \\ \sin \beta_{31} \\ \cos \beta_{31} \end{pmatrix}. \tag{9}$$

To get the direction vector of this line, as seen from the local coordinate system of the third projection, we have to multiply this direction vector with the rotation matrix that describes the α and the β rotations towards the $\hat{D}_3$ direction:

$$\begin{pmatrix} \cos \beta_3 \cos \alpha_3 & \cos \beta_3 \sin \alpha_3 & -\sin \beta_3 \\ -\sin \alpha_3 & \cos \alpha_3 & 0 \\ \sin \beta_3 \cos \alpha_3 & \sin \beta_3 \sin \alpha_3 & \cos \beta_3 \end{pmatrix} \begin{pmatrix} 0 \\ \sin \beta_{31} \\ \cos \beta_{31} \end{pmatrix}$$
$$= \begin{pmatrix} \cos \beta_3 \sin \alpha_3 \sin \beta_{31} - \sin \beta_3 \cos \beta_{31} \\ \cos \alpha_3 \sin \beta_{31} \\ \sin \beta_3 \sin \alpha_3 \sin \beta_{31} + \cos \beta_3 \cos \beta_{31} \end{pmatrix}. \tag{10}$$

Apart from the γ_3 rotation, this then brings this vector to the local coordinate system of the third projection. This vector lies in the X–Y plane of that coordinate system, and the z-coordinate of this vector must thus be zero. The vector will be of the type:

$$\hat{C}'_{31} = \begin{pmatrix} \cos \theta \\ \sin \theta \\ 0 \end{pmatrix}. \tag{11}$$

Since everything about the vector is known we can readily calculate the angle θ. We had used the third projection to find the direction of the third common line ($\hat{C}_{31}$) in the first place, so we know what its direction ϕ in the real local coordinate system (including the local γ_3) is. The rotation between these two directions ($\phi - \theta$) give us the missing γ_3 angle.

3. Discussion

Methods for finding the relative spatial orientations of different projection images already have a history in electron microscopy. They have, however, mainly been techniques that in some form exploit a

priori information. For example, the relative orientation of two projection images of a two-dimensional crystal may be determined by comparing the reciprocal lattice vectors of both images with each other. Relative orientations between projections may also be determined by triangulation of small high-contrast markers that can be identified unambiguously in different projections or some other form of a priori information [22].

The earlier technique that is closest to the method presented here is that of "common lines" proposed by Crowther et al. [17,18] for structures with a high degree of symmetry. It has hitherto been applied to icosahedral viruses exclusively. The reason for this is that a general projection of an icosahedral structure appears 60 times in the structure. Thus, each general central section will intersect with 59 different copies of itself leading to 59 common lines (one of which degenerates to a full plane). This redundancy, in turn, gives ample opportunity to suppress the noise present in the original image [17,18] even without having to average different individual molecular images. Interestingly, the common lines technique requires a minimum pointgroup symmetry of C3, since in such a structure each general projection will intersect with two symmetry-related central sections leading to two common lines per projection. This is the minimum necessary and corresponds to the minimum of three different projections needed to orient an asymmetric object with the angular reconstitution approach. A general C2 pointgroup projection will only have one common line with its symmetry-related version, which is insufficient to orient the projection using the common lines technique. A minimum of two different projections are needed to orient general projections of a C2 pointgroup molecule with angular reconstitution. For symmetric objects, we also have to investigate the SCF of each projection with itself.

Two techniques have been proposed to deal with randomly oriented particles that rely heavily on the use of spherical harmonics. The first technique was proposed by Kam and coworkers [23,24] and was shown to work on model data. Their technique, which incorporates an interesting but complicated method of gathering the 3D information, explicitly requires the molecular projections to be randomly and uniformly distributed over all possible orientations. This requirement may be difficult to fulfill in practice (see, however, ref. [24]).

The technique proposed by Provencher and Vogel [25,26], is designed to orient, in a least-squares fashion, a set of limited-angle tilt series of different individual particles relative to each other, or alternatively, orient different views of a highly symmetrical object like an icosahedral virus [26]. It is still too early to fully compare the relative merits of the methods, yet it is probably justified to conclude that this method, in which the object is decomposed into (3D) orthogonal functions, implicitly requires the 3D volume to be filled rather homogeneously and thus requires the input projections to be evenly distributed over all possible orientations.

Iterative techniques have also been proposed [27–29] in which the object is first reconstructed using random or roughly estimated angular assignments. The first reconstruction is then projected out again, and the reprojections are used to refine the angular assignments of the original projections. The technique is based on the self-consistency of the reconstruction and will only work when a sufficiently large number of projections is available.

A problem with all techniques is the assumption that the projections are all of the same object. With negative stain preparations, the stain distribution may depend on the orientation of the molecule relative to the carbon foil, and that requirement may not always be strictly fulfilled. In particular the stain surrounding the molecule may be disturbing , and we thus use very narrow contour masks to suppress the disturbing influence of the surrounding stain. An advantage of the techniques, on the other hand, is that flattening of the molecules in the (projection) direction on the carbon foil [30] does not disturb the projection to a first approximation. Perhaps the greatest advantage of the techniques – especially if no additional tilting is required – is that each molecule is only exposed once to the electron radiation, such that low dose techniques [31,32] can be realised.

In virtually all sets of molecular images that have been analyzed, including hemocyanins [11,33,34] and

ribosomal subunits [13,35–37], a clear partitioning into just a few different characteristic views was observed. With just a limited number of projections, we can use the angular reconstitution technique to determine the relative orientation, yet the attainable resolution in a reconstruction is then also limited [15,38]. Additional tilting over small angles may thus be necessary to achieve a more uniform distribution of information in 3D Fourier space. In situations in which high resolution is needed but only very few projections are available, a combination of the reconstitution technique with the "conical" single tilt technique by Radermacher and Frank [39] may be the best way to proceed. Alternative specimen preparation techniques such as embedding the molecules in a thin layer of vitreous ice [40,26] may lead to a greater randomness of the molecular orientations and thus eventually to a higher resolution in the reconstruction.

The angular reconstitution algorithm is essentially an algorithm for direct 3D applications, since the projections may not be related by a single tilt axis. Direct 3D reconstruction algorithms thus have to be applied for the reconstruction once the angles have been determined. These may operate in real space [28], such as the "exact" filtered backprojection algorithm [41] or in Fourier space. As is generally the case, we cannot determine the handedness of the object, without explicitly knowing some specific tilt direction [21]. With the angular reconstitution method, we obtain two correct reconstructions which are mirror-related to each other. Independent handedness information is thus needed.

Throughout this paper the projections were implicitly assumed to be centered so that no translation in the plane of the projection was needed. That will, however, not be the case normally and we have to center the projections prior to the angular reconstitution. The obvious candidate technique for this purpose is alignment of the centre of mass of the projections, since the center of mass of a projection is the projection of the 3D center of mass of the object. When more than three projections are available (asymmetric object) we can use the three first projections to orient all other available projections. All image processing mentioned in this paper was performed in the framework of the IMAGIC image processing system [33]

4. Conclusions

The angular reconstitution method proposed in this paper allows the a posteriori determination of the relative orientation of a set of two-dimensional images obtained by projecting a three-dimensional object in different directions. The technique may be applied both to symmetric and asymmetric objects. The bottleneck that has, for many years, prevented the more general application of such reconstruction techniques to electron microscopical images of "randomly oriented" biological macromolecules was the inherently very poor signal-to-noise ratio (SNR) of such images. With the new multivariate statistical classification techniques [11,12], however, we can now extract good SNR characteristic views [13] from noisy, mixed populations of images. The proposed angular reconstitution technique can potentially be applied to a large variety of problems of structure determination of biological macromolecules. From the point of view of specimen preparation, single molecule preparations are very easy to obtain. For asymmetric objects the minimum requirement for the determination of the relative Euler angles are three projections which are NOT related by rotation around a single axis.

Acknowledgements
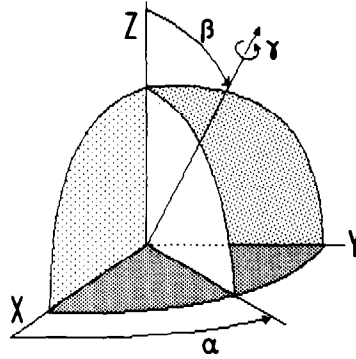
Fig. 6. Definition of Euler angles used in this paper, relative to a conventional right-handed $X-Y-Z$ coordinate system.

Appendix

We define the Euler angles and the associated rotation matrices used in this paper; some further elementary operations are listed. Euler angles (fig. 6) are defined as three subsequent rotations of the coordinate system, each of which can be described by a separate rotation matrix. The net effect of the three rotations is given by the matrix product of the three rotation matrices. The first rotation angle α describes a positive (counterclockwise) rotation of the $X-Y-Z$ system around the Z-axis. We then rotate counterclockwise around the new Y-axis over the angle β, which leads to a rotation of the Z-axis away from its original position. Finally, the rotation over the angle γ is a counterclockwise rotation around the new Z-axis. The three subsequent rotations may be described by the rotation matrices:

$$R = R_\gamma R_\beta R_\alpha \tag{A.1}$$

$$= \begin{pmatrix} \cos\gamma & \sin\gamma & 0 \\ -\sin\gamma & \cos\gamma & 0 \\ 0 & 0 & 1 \end{pmatrix} \begin{pmatrix} \cos\beta & 0 & -\sin\beta \\ 0 & 1 & 0 \\ \sin\beta & 0 & \cos\beta \end{pmatrix} \begin{pmatrix} \cos\alpha & \sin\alpha & 0 \\ -\sin\alpha & \cos\alpha & 0 \\ 0 & 0 & 1 \end{pmatrix} \tag{A.2}$$

$$= \begin{pmatrix} \cos\gamma & \sin\gamma & 0 \\ -\sin\gamma & \cos\gamma & 0 \\ 0 & 0 & 1 \end{pmatrix} \begin{pmatrix} \cos\beta\cos\alpha & \cos\beta\sin\alpha & -\sin\beta \\ -\sin\alpha & \cos\alpha & 0 \\ \sin\beta\cos\alpha & \sin\beta\sin\alpha & \cos\beta \end{pmatrix} \tag{A.3}$$

$$= \begin{pmatrix} \cos\gamma\cos\beta\cos\alpha - \sin\gamma\sin\alpha & \cos\gamma\cos\beta\cos\alpha + \sin\gamma\cos\alpha & -\cos\gamma\sin\beta \\ -\sin\gamma\cos\beta\cos\alpha - \cos\gamma\sin\alpha & -\sin\gamma\cos\beta\sin\alpha + \cos\gamma\cos\alpha & \sin\gamma\sin\beta \\ \sin\beta\cos\alpha & \sin\beta\sin\alpha & \cos\beta \end{pmatrix}. \tag{A.4}$$

The rotation matrix R rotates the $X-Y-Z$ coordinate system to a $X'-Y'-Z'$ coordinate system. The rotation matrix that rotates the $X'-Y'-Z'$ back to the $X-Y-Z$ system is the inverse of R, which at the same time is the transposed of R $(= R')$, since the rotation is a unitary transformation. The transposed R' is also equal to the matrix product:

$$R' = R'_\alpha R'_\beta R'_\gamma. \tag{A.5}$$

That this is indeed the inverse of the R matrix can readily be verified by working out (I is the unit matrix):

$$R'R = R'_\alpha R'_\beta R'_\gamma R_\gamma R_\beta R_\alpha = I. \tag{A.6}$$

This implies that what is a γ-rotation in one system corresponds to an α-rotation in the inverse system and vice versa. The direction vector corresponding to the (α, β) direction is, as can be verified with the help of fig. 6:

$$\hat{D}_{\alpha,\beta} = \begin{pmatrix} \sin \beta \cos \alpha \\ \sin \beta \sin \alpha \\ \cos \beta \end{pmatrix}. \tag{A.7}$$

For completeness, the definitions of inner and outer products between two vectors are also repeated here. The inner or scalar product $\overline{A} \cdot \overline{B}$:

$$\overline{A} \cdot \overline{B} = \begin{pmatrix} a_1 \\ a_2 \\ a_3 \end{pmatrix} \cdot \begin{pmatrix} b_1 \\ b_2 \\ b_3 \end{pmatrix} = a_1 \cdot b_1 + a_2 \cdot b_2 + a_3 \cdot b_3, \tag{A.8}$$

and the outer or vector product $A \times B$:

$$\overline{A} \times \overline{B} = \begin{pmatrix} a_1 \\ a_2 \\ a_3 \end{pmatrix} \times \begin{pmatrix} b_1 \\ b_2 \\ b_3 \end{pmatrix} = \begin{pmatrix} a_2 \cdot b_3 - a_3 \cdot b_2 \\ a_3 \cdot b_1 - a_1 \cdot b_3 \\ a_1 \cdot b_2 - a_2 \cdot b_1 \end{pmatrix} = \overline{C}. \tag{A.9}$$

Note: the result of the vector product between A and B, C, is always perpendicular to both A and B. Moreover, if both A and B are unit vectors, the inner product $A \cdot B$ is identical to the cosine of the angle between A and B.

References

[1] R.A. Brooks and G. di Chiro, Phys. Med. Biol. 21 (1976) 689.
[2] R.A. Crowther and A. Klug, Structure analysis of macromolecular assemblies by image reconstruction from electron micrographs, in: Annual Review of Biochemistry, Vol. 44, Ed. E.E. Snell (1975) pp. 161–182.
[3] J. Frank, Three-dimensional reconstruction of single molecules, in: Methods in Cell Biology, Vol. 22, Three-Dimensional Ultrastructure in Biology, Ed. J.N. Turner (Academic Press, New York, 1981) pp. 325–344.
[4] U. Aebi, W.E. Fowler and P.R. Smith, Ultramicroscopy 8 (1982) 191.
[5] U. Aebi, W.E. Fowler, E.L. Buhle and P.R. Smith, J. Ultrastruct. Res. 88 (1984) 143.
[6] W. Hoppe, J. Gassmann, N. Hunsmann, H.J. Schramm and M. Sturm, Hoppe-Seyler's Z. Physiol. Chem. 355 (1974) 1483.
[7] R. Henderson and P.N.T. Unwin, Nature 257 (1975) 28.
[8] V. Knauer, R. Hegerl and W. Hoppe, J. Mol. Biol. 163 (1983) 409.
[9] H. Oettl. R. Hegerl and W. Hoppe, J. Mol. Biol. 163 (1983) 431.
[10] L. Lebart, A. Morineau and K.M. Warwick, Multivariate Descriptive Statistical Analysis (Wiley, New York, 1984).
[11] M. van Heel and J. Frank, Ultramicroscopy 6 (1981) 187.
[12] M. van Heel, Ultramicroscopy 13 (1984) 165.
[13] M. van Heel and M. Stoeffler-Meilicke, EMBO J. 4 (1985) 2389.
[14] D.J. DeRosier and A. Klug, Nature 217 (1968) 130.
[15] R.A. Crowther, D.J. DeRosier and A. Klug, Proc. Roy. Soc. (London) A317 (1970) 319.
[16] D.J. DeRosier and P.B. Moore, J. Mol. Biol. 52 (1970) 355.
[17] R.A. Crowther, L.A. Amos, J.T. Finch, D.J. DeRosier and A. Klug, Nature 226 (1970) 421.
[18] R.A. Crowther, Phil. Trans. Roy. Soc. London B261 (1971) 221.
[19] B.W. Matthew and S.A. Bernhard, Ann. Rev. Biophys. Bioeng. 2 (1973) 257.
[20] I.N. Bronstein and K.A. Semendjajew, Taschenbuch der Mathematik (Harri Deutsch, 1977) pp. 163–165.
[21] A. Klug and J.T. Finch, J. Mol. Biol 31 (1968) 1.
[22] G. Harauz and F.P. Ottensmeyer, Science 226 (1984) 936.
[23] Z. Kam, J. Theoret. Biol. 82 (1980) 15.

[24] Z. Kam and I. Gafni, Ultramicroscopy 17 (1985) 251.

[25] S.W. Provencher and R.H. Vogel, Regularization techniques for inverse problems in molecular biology, in: Numerical Treatment of Inverse Problems in Differential and Integral Equations, Eds. F. Deulflhard and E. Hairer (Birkhauser, Basel, 1983).

[26] R.H. Vogel, S.W. Provencher, C.-H. von Bonsdorff, M. Adrian and J. Dubochet, Nature 320 (1986) 533.

[27] M. van Heel, Three-dimensional reconstruction from projections with unknown angular relationships, in: Proc. 8th European Congr. on Electron Microscopy, Budapest, 1984, pp. 1347–1348.

[28] G. Harauz and F.P. Ottensmeyer, Ultramicroscopy 12 (1984) 309.

[29] G. Harauz and M. van Heel, Direct 3D reconstruction from projections with initially unknown angles, in: Pattern Recognition in Practice II, Eds. E.S. Gelsema and L.N. Kanal (North-Holland, Amsterdam, 1986).

[30] E. Kellenberger, M. Haener and M. Wurtz, Ultramicroscopy 9 (1982) 139.

[31] P.N.T. Unwin and R. Henderson, J. Mol. Biol. 94 (1975) 425.

[32] R. Henderson, J.M. Baldwin, K.H. Downing, J. Lepault and F. Zemlin, Ultramicroscopy 19 (1986) 147.

[33] M. van Heel and W. Keegstra, Ultramicroscopy 7 (1981) 113.

[34] M.M.C. Bijlholt, M.G. van Heel and E.F.J. van Bruggen, J. Mol. Biol. 161 (1982) 139.

[35] J. Frank, A. Verschoor and M. Boublik, Science 214 (1981) 1353.

[36] J. Frank, A. Verschoor and M. Boublik, J. Mol. Biol. 161 (1982) 107.

[37] G. Harauz, E.J. Boekema and M. van Heel, Statistical image analysis of electron micrographs of ribosomal subunits, in: Methods in Enzymology (Academic Press, Orlando, FL, in press).

[38] M. van Heel and G. Harauz, Optik 73 (1986) 119.

[39] M. Radermacher, T. Wagenknecht, A. Verschoor and J. Frank, 3D reconstruction of the 50S ribosomal subunit of escherichia coli, in: Proc. 44th Annual EMSA Meeting, Albuquerque, NM, 1986, Ed. G.W. Bailey (San Francisco Press, 1986) pp. 40–41.

[40] M. Adrian, J. Dubochet, J. Lepault and A.W. McDowall, Nature 308 (1984) 32.

[41] G. Harauz and M. van Heel, Optik 73 (1986) 146.